# Water Vapor Pressure Model for Cloud Vertical Structure Detection in Tropical Region

Feng Yuan, *Student Member, IEEE*, Yee Hui Lee, *Senior Member, IEEE*, Yu Song Meng, *Member, IEEE*, and Jin Teong Ong

***Abstract*—A new method using water vapor pressure (WVP) from a radiosonde profile to determine the cloud vertical structure for the tropical region is proposed in this paper. This includes both the cloud base height and the cloud occurrences at different levels in the atmosphere. Our study shows that the presence of clouds depends on the following criterion: the measured WVP is larger than the critical WVP at the same level. The applicable level is found to be within the range of 300–12 000 m. The estimated cloud vertical structure using the proposed method is compared with the Salonen and Uppala (SU) model, the ceilometer data, and two kinds of meteorological observation data, namely, SYNOP and METAR. The proposed model shows a higher accuracy level of prediction of the cloud vertical structure as compared with the existing SU model.**

***Index Terms*—Ceilometer, cloud base height (CBH), cloud vertical structure, radiosonde, water vapor pressure (WVP).**

## I. Introduction

CLOUD plays a significant role in both the Earth's climate system [1], [2] and the ground-to-space radio communication system [3]. By influencing the hydrological cycle and the radiation balance [4], [5], it can cause a wide variation in weather conditions. Cloud can also cause severe impairment to satellite communications, particularly for low-margin systems [6] such as the very small aperture terminal operating in the Ka-band (20/30 GHz) or above. Moreover, absorption from cloud constituents can affect some sensors working in the visible and near-infrared range of the electromagnetic spectrum [7]. These effects are even more severe in the tropical region (e.g., Singapore) due to the high probability for the occurrence of convective clouds. Unlike clouds found in other subtropical and temperate regions, these convective clouds are cumulus, extending over high vertical altitudes, and are heavy in liquid water content [8]. Therefore, cloud detection becomes a very important issue for a wide range of remote-sensing applications.

Manuscript received May 13, 2015; revised January 27, 2016 and March 7, 2016; accepted May 18, 2016. This work was supported by the Defence Science and Technology Agency, Singapore.

F. Yuan and Y. H. Lee are with the School of Electrical and Electronic Engineering, Nanyang Technological University, Singapore 639798 (e-mail: yuan0053@e.ntu.edu.sg; eyhlee@ntu.edu.sg).

Y. S. Meng is with the National Metrology Centre, Agency for Science, Technology and Research (A*STAR), Singapore 118221 (e-mail: ysmeng@ieee.org; meng_yusong@nmc.a-star.edu.sg).

J. T. Ong is with C2N Pte. Ltd., Singapore 199098.

Color versions of one or more of the figures in this paper are available online at http://ieeexplore.ieee.org.

Digital Object Identifier 10.1109/TGRS.2016.2574744

Radio-sounding observation data have been widely applied to model the cloud vertical structure [9]–[12], since it is implemented with various sensors to measure important meteorological variables such as temperature, pressure, and relative humidity (RH) along a vertical path. To determine the cloud base height (CBH), ceilometer is sometimes used [13]–[17]; meteorological surface observations are also effective for CBH and cloud coverage determination [18], [19].

Decker *et al.* [9] proposed the use of certain RH as a constant threshold to detect the CBH and cloud thickness in 1978. CBHs were determined at such level when the RH first exceeded 95%, and the cloud thickness was determined using the points at which the RH dropped below 95% along the same cloud layer. In 1995, after comparing the ceilometer measurements of CBH with radiosonde humidity profiles, Han and Westwater revised this constant RH threshold to 90% [10] to make the two types of existing data have better agreement. In 1995, Wang and Rossow [11] proposed a method with three RH criteria to identify the cloud vertical structure: maximum RH in a cloud of at least 87%, minimum RH of at least 84%, and RH jumps exceeding 3% at cloud-layer top and base.

Another typical approach for cloud detection applied by Salonen and Uppala (SU) [12] in 1991 used a pressure-dependent critical humidity function to detect the presence of cloud. It is noted that all the existing cloud detection models previously mentioned are based only on the RH profiles as a threshold.

Water vapor plays an important role for the hydrological cycle in the Earth [20]. It evaporates from river, lake, or sea surface and then condenses to form clouds. Blown by the winds, clouds change their shape and move to other places. Finally, they will precipitate in the form of rain and/or snow, thus falling back onto the Earth's surface. The amount of water vapor suspended in the air and the temperatures of water vapor are the two key factors contributing to the formation of clouds. Water vapor pressure (WVP) relying on these key factors should have some positive correlation with the cloud.

Therefore, in this paper, as a continuation of the work in [21], we will propose an alternative approach for determining the cloud vertical structure, using WVP along the path to detect the presence of cloud.

In the following, Section II provides a description of two popular cloud detection models, which illustrates the different critical humidity thresholds and criteria for cloud detection. The meteorological data (radiosonde profiles, surface cloud observation data, ceilometer data, and hourly surface report) are introduced in Section III. Section IV presents our proposed

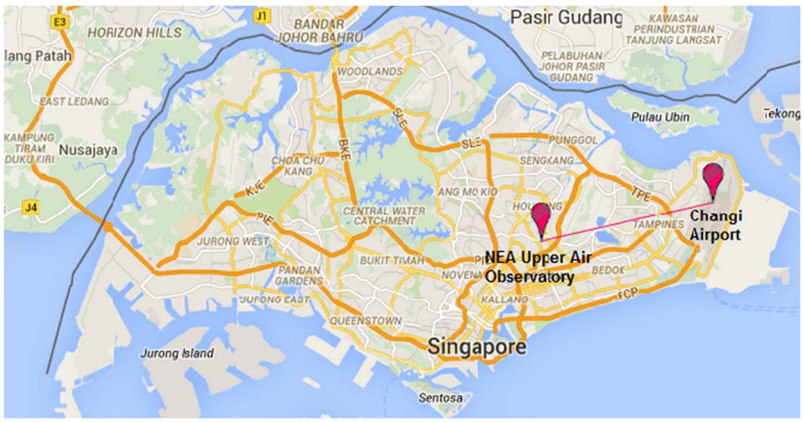


Fig. 1. Site difference between the NEA Upper Air Observatory and the Changi Airport.

methodology for modeling the cloud vertical structure using WVP. A performance evaluation of the proposed WVP model is given in Section V. Finally, conclusions are presented in Section VI.

## II. Cloud Detection Models

Two popular cloud detection models are introduced below with different critical humidity thresholds and criteria for cloud detection, namely, the SU model and the Decker model.

### A. SU Model

The SU model [12] has been adopted in ITU-R P.840-6 [22] owing to its solid physical basis. It identifies a cloud when the measured RH from radiosonde exceeds the critical humidity function $\mathrm{RH}_c$ as follows:

$$\mathrm{RH}_c = 1 - \alpha\sigma(1-\sigma)\left[1+\beta(\sigma-0.5)\right] \tag{1}$$

where $\sigma = P(i)/P(0)$, and $P(i)$ and $P(0)$ are the respective pressures (hPa) at the considered $i$th atmospheric level and at the ground level. $\alpha$ and $\beta$ are two empirical parameters where $\alpha = 1.0$ and $\beta = \sqrt{3}$ in [12]. The work in [23] reported that the SU model is the best model for estimating cloud attenuation over equatorial climate based on their measurements and analysis and, therefore, will be used for comparison purposes.

### B. Decker Model

The Decker model [9] is a direct and simple way for the identification of clouds from the atmospheric profiles. By comparing the RH profile with a constant threshold, the cloud vertical structure can be determined. The suggested threshold in the earlier work of Decker was 95% (De95) [9], whereas in a recent work, the suggested threshold was 90% (De90) [10]. Cloud layers are identified in the profile when the atmospheric RH exceeds the RH threshold. In the following, both the models will be compared with our proposed method and the existing meteorological data sets.

## III. Meteorological Data

Four types of meteorological data sets are used for comparison on the cloud vertical structure. Radiosonde data are used to detect the cloud vertical structure based on models. The ceilometer data and two sets of observation data, namely, SYNOP and METAR, provide the cloud occurrences at different levels and the first-layer CBH for the performance evaluations of the models.

### A. Radiosonde Data

Radiosonde data are acquired from an online database provided by the Department of Atmospheric Science, University of Wyoming [24].

For the Singapore station, WSSS, the raw experimental data are collected by the National Environment Agency (NEA) at the Singapore Upper Air Observatory (1.34°N, 103.89°E), Station Number 48698 in the World Meteorological Organization (WMO) network shown in Fig. 1. From our previous work [25], the online radiosonde data have proved feasible for the evaluation of cloud attenuation in the tropical region. The radiosonde observation times are approximately 00:00 UTC and 10:00 UTC, twice per day.

The RH, temperature, and altitude data from radiosonde are used to estimate the WVP for cloud detection. The maximum altitude of the radiosonde data can be up to 50 000 m, which is limited by the instrument. However, most of the time, RH data are only available up to around 12 000 m. Therefore, for cloud detection, the maximum detectable cloud will be up to 12 000 m. Above this level, the clouds are usually full of ice crystals.

To derive a cloud detection model suitable for the tropical region, the radiosonde data from nine tropical stations, each station for the years 2010–2013, i.e., a total of 36 years, are acquired from the online database. The nine stations are chosen to be within ±20° latitude with high availability of data, which is approximately 95% availability for the nine stations for the four years in this study. The nine stations with their corresponding locations are given in Table I.

### B. Ceilometer Data

The ceilometer (by the CL31 model) data set is used to validate the CBH determined by the models. The data set is collected at the Changi Airport office of NEA (1.37°N, 103.98°E),

TABLE I
NINE RADIOSONDE STATIONS SELECTED IN THE TROPICAL REGION

| Station ID | Location | Lat. | Lon. |
|---|---|---|---|
| WAAA | Hasanuddin Ujung AB, Indonesia | 5.06°S | 119.5°E |
| WSSS | NEA Upper Air Observatory, Singapore | 1.34°N | 103.89°E |
| WIMM | Medan Polonia MIL, Indonesia | 3.57°N | 98.68°E |
| DIAP | Abidjan, Cote d'Ivoire | 5.25°N | 3.93°W |
| VOMM | Madras Minambak, India | 13.00°N | 80.18°E |
| MMAA | Acapulco G. Alvarez, Mexico | 16.77°N | 99.75°W |
| MKJP | Norman Manley Kings, Jamaica | 17.93°N | 76.78°W |
| MDSD | Caucedo De Las Amer, Dominican Republic | 18.43°N | 69.67°W |
| MWCR | Owen Roberts Intl., Cayman Islands | 19.28°N | 81.35°W |

TABLE II
CODE DESCRIPTION FOR CBH IN SYNOP

| Code figure | Cloud base height |
|---|---|
| 0 | 0 to 50 m |
| 1 | 50 to 100 m |
| 2 | 100 to 200 m |
| 3 | 200 to 300 m |
| 4 | 300 to 600 m |
| 5 | 600 to 1000 m |
| 6 | 1000 to 1500 m |
| 7 | 1500 to 2000 m |
| 8 | 2000 to 2500 m |
| 9 | 2500 m or more |
| / | Base height of cloud not known |

as shown in Fig. 1. They are continuously recorded at a time interval of 1 min with a vertical resolution of 5 m. Although ceilometer can provide CBH information up to three layers, the available information of the upper two layers is very limited. Therefore, only the CBHs for the first layer at approximately 00:00 UTC and 10:00 UTC are used.

### C. Human Observations

The human observation data set is obtained from the SYNOP report also collected by the NEA Upper Air Observatory in Singapore, at the same time and location as the radiosonde data. SYNOP is a numerical code (called FM-12 by WMO) used for reporting weather observations made by weather stations. The data include cloud coverage, first-layer CBH, and types of clouds at different levels. The data for cloud type at the low level, middle level, and high level are processed for indicating the cloud occurrences at each level. The first-layer CBH is used to verify the accuracy of the models. The data are encoded as a code figure, as shown in Table II. It is noted that the performance of ceilometer [26] has been also checked against the human observations by the manufacturer.

### D. Hourly Surface Report

Hourly surface reports (i.e., METAR report in this study) can be also obtained from the database provided by the University of Wyoming [24]. The raw data are collected at the Changi Airport office of NEA (same as ceilometer). Raw data include cloud coverage and cloud height information at different levels with an interval of half an hour for Singapore. The cloud data are also processed so as to allow for the comparison of cloud occurrence at low, middle, and high levels.

## IV. METHODOLOGY

Since the condensation of water vapor is a source of cloud formation, the correlation of the WVP (affecting the condensation and evaporation of water vapor) with the cloud vertical structure should be very obvious. Thereby, WVP can be a good parameter for cloud detection.

To determine the WVP at different atmospheric levels, RH and temperature data from radiosonde vertical profiles are used for calculating the spatial pressure of water vapor [27], [28], i.e.,

$$e = \mathrm{RH} \times \exp(-37.2465 + 0.213166T - 2.56908 \times 10^{-4}T^2) \tag{2}$$

where $e$ stands for the WVP in hectopascals, and $T$ is the absolute temperature in degrees Kelvin.

An example of WVP at different levels is shown in Fig. 2(a). It can be easily observed that WVP has a negative exponential relationship with altitude. To properly and accurately estimate the exponential relationship, 36 years of radiosonde data (a total of 891 710 data points) collected at nine different locations in the tropical region have been processed using a regression technique. Fig. 2(b) presents the variation of WVP versus altitude. It can be observed that below around 12 000 m, the WVPs have large variations. This variation is due to the change in RH and temperature on different days, which could indicate the appearance of cloud.

A critical WVP function [red solid line in Fig. 2(b)] for cloud detection is determined by applying the exponential curve-fitting technique on the dependent variable (WVP) and the independent variable (altitude) in the form of

$$e_c = a \cdot \exp(b \cdot \mathrm{Alt}) \tag{3}$$

where Alt is the altitude in meters, and $e_c$ is the critical WVP threshold in hectopascals in this study. Through the least squares regression technique, empirical values for the two parameters $a$ and $b$ are derived to be 28.81 and $-0.0004363$.

The criterion of cloud detection proposed in this study is: *if the measured WVP is larger than the critical WVP threshold given in* (3) *at the same level, this level is assumed to be in cloud*.

Wang and Rossow [11] have reported that if the detected cloud base is lower than 500 m above the ground level, the cloud layer shall be discarded. However, for the tropical region, the seasonal low-level CBHs are found to vary from 356 to 820 m, as reported in [29]. Therefore, the baseline of 500 m as reported in [11] may be too high and will be adjusted to about 300 m for our cloud detection model. Furthermore, since most of WVP variations are below around 12 000 m, an upper applicable range of 12 000 m is assumed.

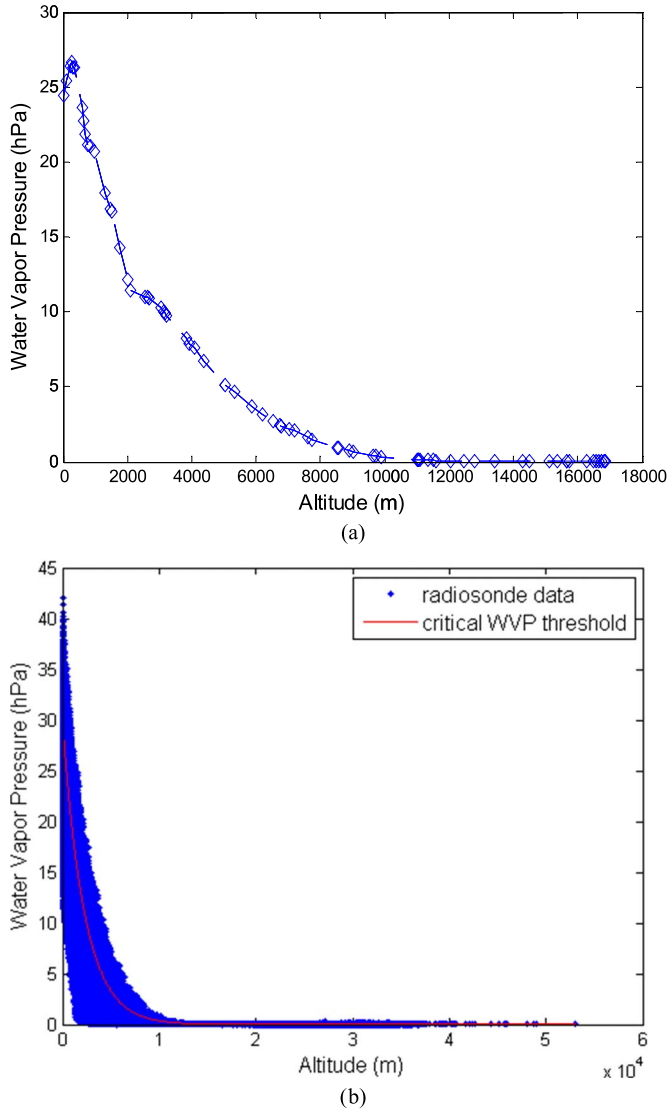


Fig. 2. WVP at different altitude levels. (a) One data set. (b) 36 years of radiosonde data collected from nine locations in the tropical region with curve fitting.

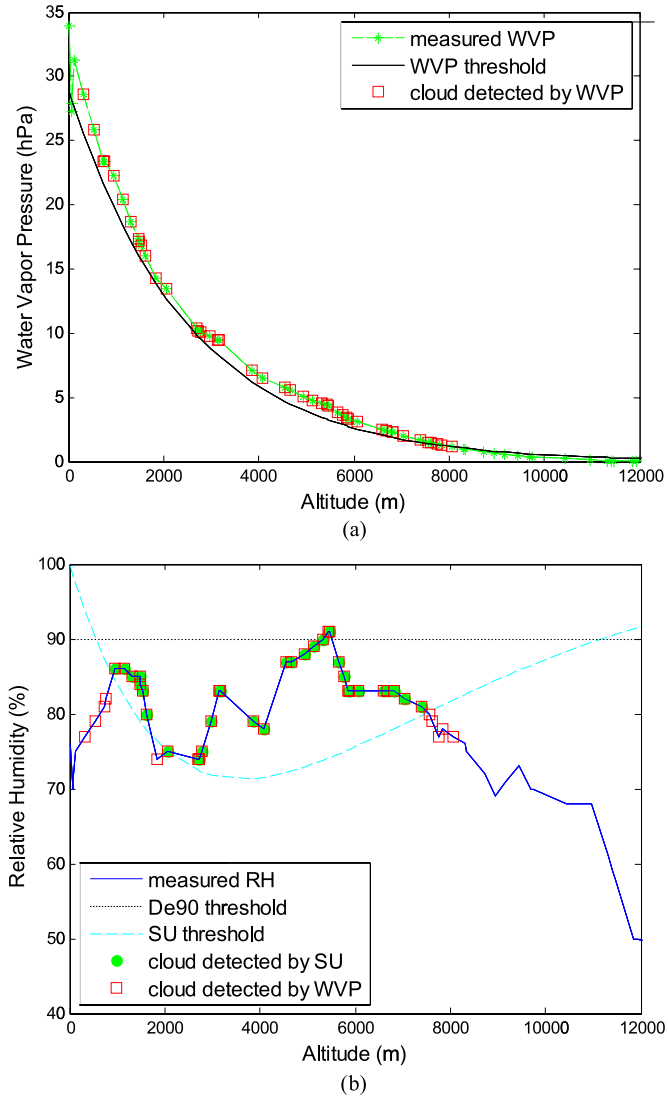


Fig. 3. Cloud vertical structure detection and comparison by the (a) WVP model, the (b) De90 model, the SU model, and the WVP model at 10:00 UTC on October 22, 2013.

In the next section, our proposed cloud detection model given in (3) will be compared and verified with existing models and meteorological data sets.

## V. Performance Evaluation

To evaluate the performance of the proposed cloud detection method, comparisons with the SU model, the De90 model, human observations, ceilometer measurements, and the hourly surface report are carried out.

### A. Cloud Vertical Structure Comparison

The detected cloud vertical structure is compared among the SU model, the De90 model, and our proposed model using the radiosonde data at same time. Fig. 3 shows an example of cloud detection at 10:00 UTC on October 22, 2013. As shown in Fig. 3(a), if the measured WVP is above the WVP threshold given by (3), it indicates that a cloud is present. The red squares represent the cloud detected by the WVP model. One thick layer of cloud can be observed in Fig. 3(a), and the cloud is from around 500 to 8000 m. Fig. 3(b) shows the cloud detected by the SU model and the De90 model. The cloud detected by the proposed WVP model as shown in Fig. 3(a) is also indicated by red squares in Fig. 3(b) for ease of comparison. For the De90 model, if the measured RH is above 90%, it indicates that a cloud is present. As shown in Fig. 3(b), the De90 model could only detect one thin layer of cloud at around 5500 m. As stated in [8], the De90 model is found to be highly inaccurate for the detection of clouds and is seldom used for the tropical region. For the SU model, if the measured RH is above the SU threshold, it indicates that a cloud is present. The cloud detected by the SU model is shown by the green dots in Fig. 3(b), i.e., low-level clouds from 1000 to 1900 m and middle-level clouds from 2000 to 7500 m. Comparing both the proposed model and the SU model, both models indicate the existence of thick clouds stretching from the low level up to the high level.

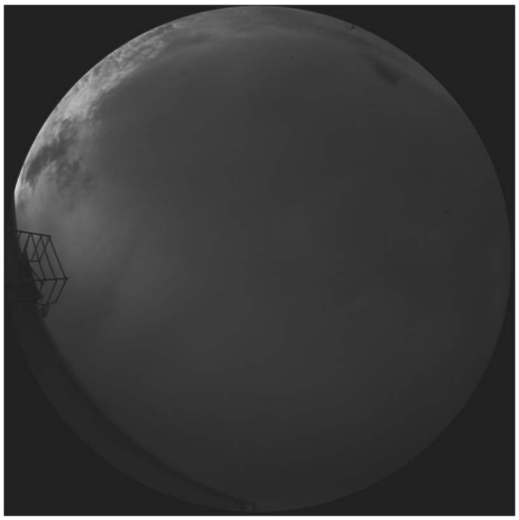

Fig. 4. Cloud image taken by the whole-sky imager at 10:00 UTC on October 22, 2013 at NTU.

However, the SU model has split the thick clouds into two layers, whereas the proposed WVP model has detected one thick layer. In addition, the CBHs and cloud top heights are also slightly different.

To further compare the performance of the three cloud detection models, cloud images taken by a whole-sky imager [30] at Nanyang Technological University (NTU) are shown in Fig. 4. It is observed that the sky is overcast with dark thick low-level cloud around the same time as the cloud detection in Fig. 3. Although there is a site difference between the radiosonde observation site and the NTU whole-sky imager site, due to the small size of the tropical country of Singapore, this heavy low-level cloud is covering the whole island. Therefore, the image can be used to show the existence of a thick low-level cloud as estimated by the empirical models of the SU model and our proposed WVP models.

### *B. Cloud Occurrence Comparison*

Cloud occurrence is classified into three categories according to the CBH above ground level. They are typically low-level cloud with CBH from 0 to 2000 m, middle-level cloud with CBH from 2000 to 5000 m, and high-level cloud with CBH above 5000 m (referred to the METAR report). The occurrences of cloud determined by the SU and WVP models are classified into the three corresponding levels previously stated for comparison purposes. For the SYNOP and METAR reports, the cloud data have already been categorized into the three different levels.

Table III shows a comparison of the percentage of cloud occurrence detected by the SYNOP and METAR reports. It should be noted that the SYNOP data are collected at the NEA Upper Air Observatory site, whereas METAR data are collected at a different location at the Changi Airport site, which are 12 km apart. It can be observed that for low-level clouds, the detection is consistent, with more than 97% of the time with clouds detected by both the SYNOP and METAR reports. This is due to the large coverage area of low-level clouds. However,

TABLE III
COMPARISON OF CLOUD OCCURRENCE BETWEEN METAR REPORT AND SYNOP REPORT *

| Low Level | | SYNOP | |
|---|---|---|---|
| | | clear sky | cloudy |
| METAR | clear sky | 0 | 0.86 |
| | cloudy | 1.86 | 97.28 |
| **Middle level** | | **SYNOP** | |
| | | clear sky | cloudy |
| METAR | clear sky | 3.15 | 55.87 |
| | cloudy | 0.86 | 40.11 |
| **High level** | | **SYNOP** | |
| | | clear sky | cloudy |
| METAR | clear sky | 1.29 | 57.74 |
| | cloudy | 1.58 | 39.40 |

* All the numbers shown in Table III are in the unit of %.

TABLE IV
COMPARISON OF CLOUD OCCURRENCE FROM MODELS (SU AND WVP) AND OBSERVATION REPORTS (SYNOP AND METAR)*

| Low level | SYNOP/METAR report | | | |
|---|---|---|---|---|
| Model | M1 | S | R | M2 |
| SU | 0.43/0.29 | 19.63/19.77 | 1.43/0.57 | 78.51/79.37 |
| WVP | 0.43/0.14 | 2.15/2.44 | 1.43/0.72 | 95.99/96.70 |
| Middle level | SYNOP/METAR report | | | |
| Model | M1 | S | R | M2 |
| SU | 0.86/6.30 | 6.88/1.43 | 3.15/52.72 | 89.11/39.54 |
| WVP | 0.43/2.58 | 2.44/0.29 | 3.58/56.45 | 93.55/40.69 |
| High level | SYNOP/METAR report | | | |
| Model | M1 | S | R | M2 |
| SU | 0.43/21.06 | 23.07/2.44 | 2.44/37.97 | 74.07/38.54 |
| WVP | 0.29/3.01 | 3.15/0.43 | 2.58/56.02 | 93.98/40.54 |

* All the numbers shown in Table IV are in the unit of %.

for middle- and high-level clouds, around 40% and 39% of the time, respectively, both reports detected clouds. This is due to the different geographical locations of the two observation sites. METAR reports being collected at the east coast of Singapore tend to experience less cloud and rain events, as reported in [31].

Table IV summarizes the percentages of matched and unmatched cloud occurrences from the two models and from the SYNOP and METAR data for the year 2013 in Singapore. The total number of observations is 698 instead of 730 due to some missing radiosonde data. The data in Table IV are discussed as follows.

i) M1 represents the percentage of the cases in which neither the models nor the SYNOP/METAR report data indicate the cloud occurrence simultaneously. For example, for 0.43% of the time, both the SU model and SYNOP data did not detect any low-level clouds, whereas for 0.29% of the time, both the SU model and the METAR data did not detect any low-level clouds. Similarly, both the proposed WVP model and the SYNOP data did not detect any low-level clouds for 0.43% of the time,

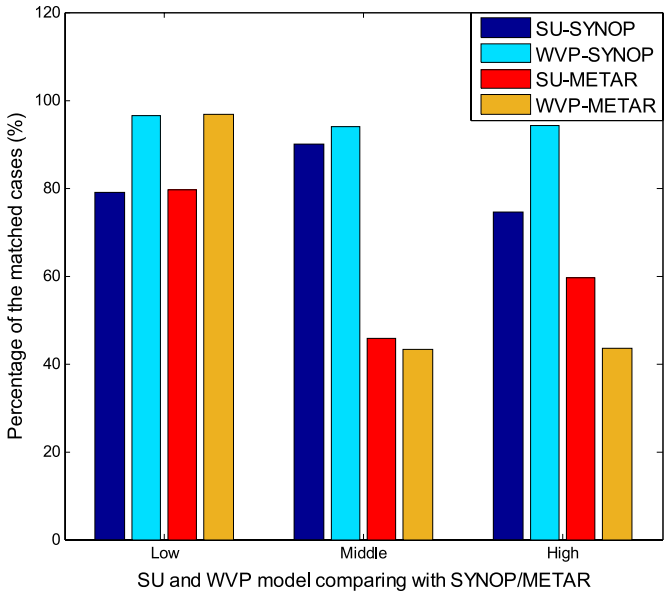


Fig. 5. Percentage of the matched cloud occurrence cases of the SU/WVP models comparing with SYNOP/METAR data.

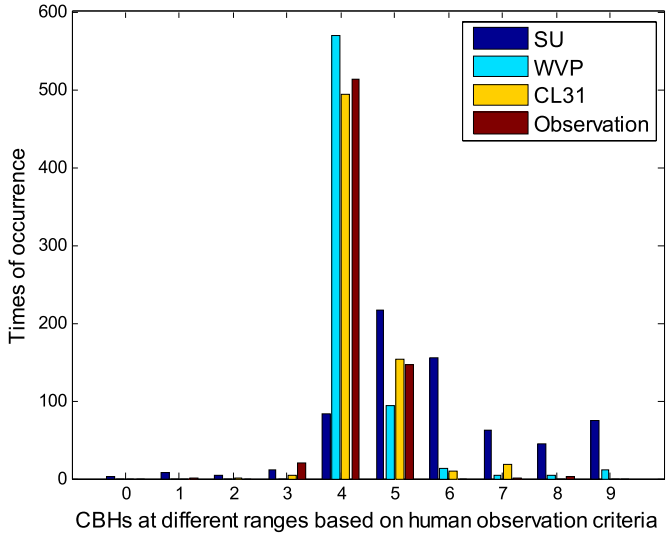


Fig. 6. Histogram of CBHs from the SU model, the WVP model, ceilometers, and human observations in 2013 in Singapore.

whereas both the WVP model and METAR data did not detect any low-level clouds for 0.14% of the time.

ii) S is the percentage of the cases in which the model does not detect any cloud while the SYNOP/METAR report data indicate a cloud.

iii) R is the percentage of the cases in which the models detect a cloud while the SYNOP/METAR report data indicate no cloud.

iv) M2 represents the percentage of the cases in which both the models and the SYNOP/METAR report data indicate cloud occurrence.

For the total matched cases, the percentage is the summation of M1 and M2; whereas for the unmatched cases, the percentage is the summation of S and R.

As observed from Table IV, for low-level cloud occurrence, the WVP model has more than 90% correct detection. To illustrate, the correct detection of the WVP model compared with the SYNOP data is $95.99\% + 0.43\% = 96.42\%$;, and the correct detection of the WVP model compared with the METAR data is $96.70\% + 0.14\% = 96.84\%$. However, the correct detection of the SU model for low-level cloud occurrence, compared with the data of the two reports, is only around 80%. This is 16% less accurate than our proposed WVP model, although both models are relatively accurate for low-level cloud detection. For middle-level cloud occurrence, the two models match the SYNOP report data well, and both have more than 90% matched cases. For high-level cloud occurrence, the two models match the SYNOP report data at about 75% for the SU model and 94% for the WVP model. The proposed WVP model has a higher accuracy level for cloud detection at the high level. However, for the METAR report data, there are fewer cases of matching between both models and METAR data as compared with the SYNOP data, as shown in Fig. 5. This is due to the difference in location between the two measurement sites (see Fig. 1). The radiosonde data used in the SU and WVP models and the SYNOP report data both are collected at the same NEA Upper Air Observatory site, whereas the METAR data are collected at the Changi Airport site (12 km away).

The conclusion can be summarized in Fig. 5. As shown, the proposed WVP model almost always compares better with the SYNOP data. This shows a higher accuracy level for cloud structure determination as compared with the existing SU model. Another conclusion is that the SYNOP data always compare better with the two models as compared with the METAR data. This is due to the geographical location of the measurement sites, which can be also observed from Table III. Note that the low-level cloud detection by both the SU model and the WVP model compared with both SYNOP and METAR data is relatively better as compared with middle- and high-level cloud detection. This might be due to the likelihood of a low-level cloud having a larger horizontal extension as compared with middle- and high-level clouds.

### C. CBH Comparison

CBHs are taken as the lowest heights estimated by the two models (the SU and WVP models), comparing with the results from the human observation and first-layer CBH from ceilometer measurements at the same time.

Fig. 6 shows one-year (2013) comparison of ceilometer measurements and human observation data, with the results estimated by the SU and WVP models in Singapore. The numbers 0–9 (same as Table II) represent different ranges according to the SYNOP human observation criteria. It is obvious that for bin 4 (300–600 m), the detected CBHs by the SU model significantly deviate from the CBHs detected/observed by the WVP model, ceilometers, and SYNOP report data. The latter three methods have very similar performance as observed. Furthermore, it can be observed that our proposed WVP have a very good agreement with the ceilometer and SYNOP report data in the range between 4 and 5 where the low-level CBHs exist most of the time.

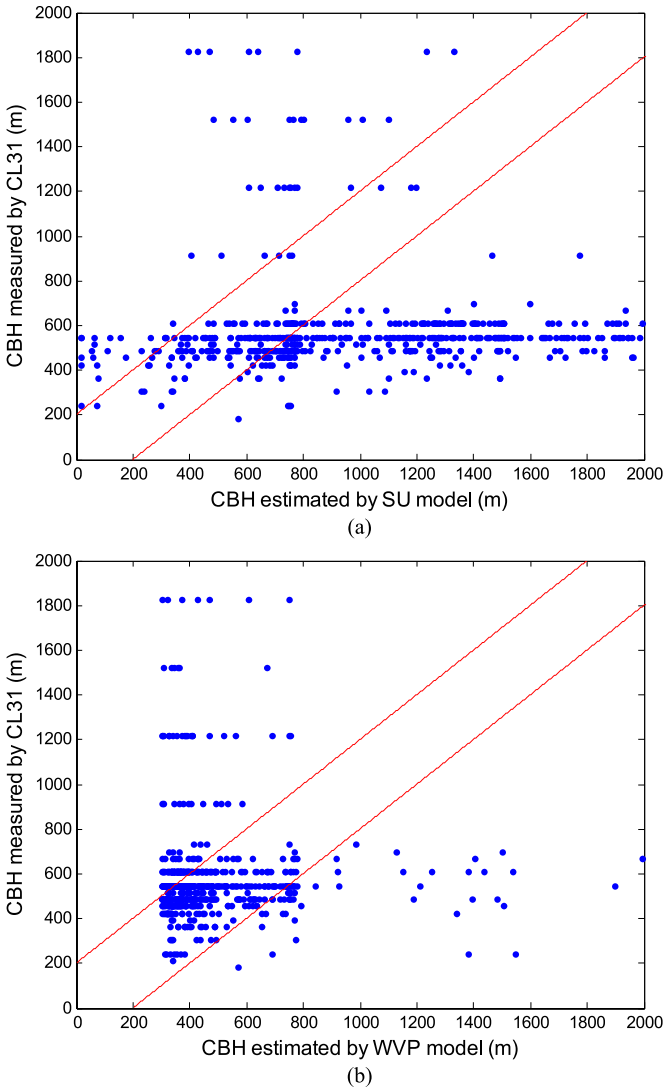


Fig. 7. Scatterplot of CBH measured by CL31 with (a) CBH estimated by the SU model and (b) CBH estimated by the WVP model.

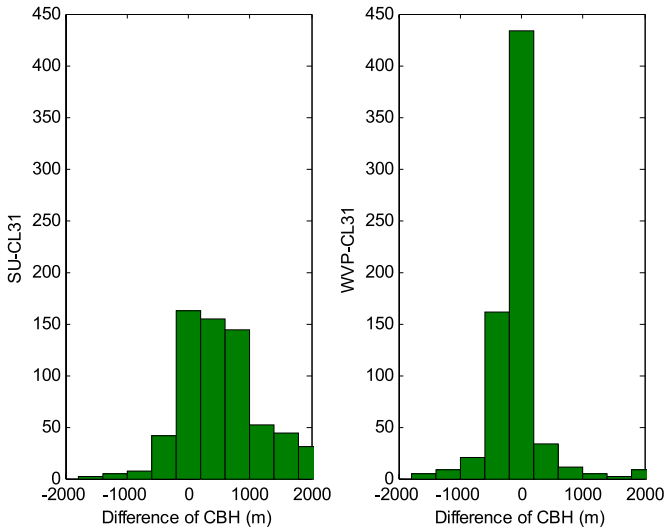


Fig. 8. Histograms of the difference between the CBHs detected by the ceilometer and the heights estimated using the SU and WVP models.

Since the ceilometer data have been widely used to verify the CBH [13]–[17], we compare the CBHs estimated by the SU model and the WVP model with ceilometer-determined CBHs. Fig. 7 shows the scatterplots of CL31 data versus the estimated CBHs for the year 2013. The upper limit of CBH is set to 2000 m since most of the CBHs (99.14% for Singapore for 2013) fall into this range. As indicated in [16], if the difference in CBH between the ceilometer data and the models is within $\pm 200$ m, the empirical models are assumed to have a correct detection.

Two red slant lines representing the detection accuracy are plotted in Fig. 7 for a clear illustration. If the CBH data fall within the range of the two lines, it is a correct detection. Fig. 7(a) shows the correlation between the results of the SU model and those of the CL31 model. It can be observed that around one-fourth of the total data is within the lines and can be regarded as correct detection. It is also observed that the SU model tends to overestimate the CBH. This is shown by the large portion of data below the lower-limit slant line. For our proposed WVP model in Fig. 7(b), it is obvious that most of the CBH data are concentrated in the range of $\pm 200$ m, within the two lines. Although there are still some falling beyond the limits, the proposed WVP model clearly has higher detection accuracy as compared with the SU model for the tropical region.

The outliers in the detection results may be due to the slight time difference of the ceilometer data and the radiosonde data. The balloon of the radiosonde needs some rising time to hit the cloud base, and this period is relatively uncertain depending on the rising velocity of the balloon, wind speed, and wind direction. Furthermore, the exact releasing time for the radiosonde is not fixed, which also leads to additional error.

Another reason might be due to the site difference (less than 12 km) between the radiosonde observation site and the ceilometer detection site, as shown in Fig. 1. If the cloud does not extend widely in the horizontal direction, detection errors will exist.

Fig. 8 shows the histograms of the actual difference between the ceilometer data and the results estimated using the two models. The bin size is set as 400 m so that the bin at zero represents a correct detection where the difference is within $\pm 200$ m. It can be observed in 2013 that the SU model has less than half a correct detection as compared with the WVP model.

To further verify our proposed WVP model, radiosonde data from other tropical regions are processed using the same procedures. Two locations in Central America, Mexico (MMAA) and Dominican Republic (MDSD) are used in this study. For these two sites, the CBHs estimated by the SU model and the WVP model are compared with the METAR CBH data for low-level clouds.

The statistical information for the correct detection of CBH (within $\pm 200$ m) by the two models is summarized in Table V. From Table V, it is found that the WVP model has more than 60% correct CBH detection, whereas the SU model has less than 30% correct CBH detection. Therefore, it can be concluded that the proposed WVP model has better detection capability than the traditional SU model and is more suitable for CBH detection within the tropical region.

TABLE V
CORRECT DETECTION RATE OF CBH FROM COMPARING SU AND WVP MODELS WITH CEILOMETER/METAR DATA

| Station ID | Correct Detection Rate | |
|---|---|---|
| | SU | WVP |
| WSSS | 22.54% | 62.75% |
| MMAA | 16.56% | 62.03% |
| MDSD | 28.02% | 62.70% |

## VI. CONCLUSION

A new method for the detection of the cloud vertical structure has been proposed in this paper. The method is based on a critical WVP model estimated from 36 sets of vertical radiosonde profiles collected from nine different locations in tropical regions over a period of four years. This model is used as a detection threshold. It applies the WVP, which is a function of both temperature and RH, instead of only the RH as is traditionally done.

The estimated results of the cloud vertical structure using our proposed WVP model are compared with the results from the SU model, ceilometer data, and two types of observation data (SYNOP and METAR). Analysis shows that the proposed WVP model is able to detect the cloud vertical structure better than the existing SU model. Through a comparison of the WVP model and the SU model on CBH estimation for other tropical countries, it is concluded that the proposed WVP model is better suited for the detection of CBH for the tropical region.

## ACKNOWLEDGMENT

The authors would like to thank the anonymous reviewers for their constructive comments and suggestions for this paper.

## REFERENCES

[1] W. B. Rossow and R. A. Schiffer, "Advances in understanding clouds from ISCCP," *Bull. Amer. Meteorol. Soc.*, vol. 80, no. 11, pp. 2261–2287, Nov. 1999.

[2] G. Hong, P. Yang, H. L. Huang, B. A. Baum, Y. Hu, and S. Platnick, "The sensitivity of ice cloud optical and microphysical passive satellite retrievals to cloud geometrical thickness," *IEEE Trans. Geosci. Remote Sens.*, vol. 45, no. 5, pp. 1315–1323, May 2007.

[3] A. D. Panagopoulos, P. M. Arapoglou, and P. G. Cottis, "Satellite communications at Ku, Ka, and V bands: Propagation impairments and mitigation techniques," *IEEE Commun. Survey Tuts.*, vol. 6, no. 3, pp. 2–14, Oct. 2004.

[4] P. Minnis *et al.*, "CERES Edition 2 cloud property retrievals using TRMM VIRS and Terra and Aqua MODIS data—Part II: Examples of averaged results and comparisons with other data," *IEEE Trans. Geosci. Remote Sens.*, vol. 49, no. 11, pp. 4401–4430, Jun. 2011.

[5] T. Maestri and R. E. Holz, "Retrieval of cloud optical properties from multiple infrared hyperspectral measurements: A methodology based on a line-by-line multiple-scattering code," *IEEE Trans. Geosci. Remote Sens.*, vol. 47, no. 8, pp. 2413–2426, Aug. 2009.

[6] A. Dissanayake, J. Allnutt, and F. Haidara, "A prediction model that combines rain attenuation and other propagation impairments along earth-satellite paths," *IEEE Trans. Antennas Propag.*, vol. 45, no. 10, pp.1546–1558, Oct. 1997.

[7] L. Gómez-Chova, G. Camps-Valls, J. Calpe-Maravilla, L. Guanter, and J. Moreno, "Cloud-screening algorithm for ENVISAT/MERIS multispectral images," *IEEE Trans. Geosci. Remote Sens.*, vol. 45, no. 12, pp. 4105–4118, Dec. 2007.

[8] F. Yuan, Y. H. Lee, and Y. S. Meng, "Comparison of cloud models for propagation studies in Ka-band satellite applications," in *Proc. 19th Int. Symp. Antennas Propag.*, Kaohsiung, Taiwan, Dec. 2014, pp. 383–384.

[9] M. T. Decker, E. R. Westwater, and F. O. Guiraud, "Experimental evaluation of ground-based microwave radiometric sensing of atmospheric temperature and water vapor profiles," *J. Appl. Meteor.*, vol. 17, no. 12, pp. 1788–1795, Dec. 1978.

[10] Y. Han and E. R. Westwater, "Remote sensing of tropospheric water vapor and cloud liquid water by integrated ground-based sensors," *J. Atmos. Ocean. Technol.*, vol. 12, pp. 1050–1059, Oct. 1995.

[11] J. H. Wang and W. B. Rossow, "Determination of cloud vertical structure from upper-air observations," *J. Appl. Meteor.*, vol. 34, no. 10, pp. 2243–2258, Oct. 1995.

[12] E. Salonen and S. Uppala, "New prediction method of cloud attenuation," *Electron. Lett.*, vol. 27, no. 12, pp. 1106–1108, Jun. 1991.

[13] M. Costa-Surós, J. Calbó, J. A. González, and J. Martin-Vide, "Behavior of cloud base height from ceilometer measurements," *Atmos. Res.*, vol. 127, pp. 64–76, Jun. 2013.

[14] T. Berendes, D. Berendes, R. Welch, E. Dutton, T. Uttal, and E. Clothiaux, "Cloud cover comparisons of the MODIS daytime cloud mask with surface instruments at the North Slope of Alaska ARM Site," *IEEE Trans. Geosci. Remote Sens.*, vol. 42, no. 11, pp. 2584–2593, Nov. 2004.

[15] M. Costa-Surós, J. Calbó, J. A. González, and C. N. Long, "Comparing the cloud vertical structure derived from several methods based on measured atmospheric profiles and active surface measurements," *Atmos. Chem. Phys. Discuss.*, vol. 13, no. 6, pp. 14 405–14 445, Jun. 2013.

[16] V. Mattioli, P. Basili, S. Bonafoni, P. Ciotti, and E. R. Westwater, "Analysis and improvements of cloud models for propagation studies," *Radio Sci.*, vol. 44, 2009, Art. no. RS2005.

[17] J. Zhang *et al.*, "Analysis of cloud layer structure in Shouxian, China using RS92 radiosonde aided by 95 GHz cloud radar," *J. Geophys. Res.*, vol. 115, no. D7, Apr. 2010.

[18] W. B. Rossow, Y. C. Zhang, and J. H. Wang, "A statistical model of cloud vertical structure based on reconciling cloud layer amounts inferred from satellites and radiosonde humidity profiles," *J. Climate*, vol. 18, no. 17, pp. 3587–3605, Sep. 2005.

[19] W. Josefsson and T. Landelius, "Effect of clouds on UV irradiance: As estimated from cloud amount, cloud type, precipitation, global radiation and sunshine duration," *J. Geophys. Res-Atmos.*, vol. 105, no. 4, pp. 4927–4935, Feb. 2000.

[20] D. Ji and J. Shi, "Water vapor retrieval over cloud cover area on land using AMSR-E and MODIS," *IEEE J. Sel. Topics Appl. Earth Observ.*, vol. 7, no. 7, pp. 3105–3116, Jul. 2014.

[21] F. Yuan, Y. H. Lee, Y. S. Meng, and J. T. Ong, "Detection of cloud vertical structure using water vapor pressure in tropical region," in *Proc. IEEE IGARSS*, Milan, Italy, pp. 906–908, Jul. 2015.

[22] "Attenuation due to clouds and fog," Int. Telecommun. Union (ITU), Geneva, Switzerland, Rec. ITU-R P.840-6, 2013.

[23] J. S. Mandeep and S. I. S. Hassan, "Cloud attenuation in millimeter wave and microwave frequencies for satellite applications over equatorial climate," *Int. J. Infrared Millimeter Waves*, vol. 29, no. 2, pp. 201–206, Feb. 2007.

[24] Department of Atmospheric Science, University of Wyoming. [Online]. Available: http://weather.uwyo.edu/upperair/sounding.html

[25] F. Yuan, Y. H. Lee, and Y. S. Meng, "Comparison of radio-sounding profiles for cloud attenuation analysis in the tropical region," in *Proc. IEEE Antennas Propag. Soc. Int. Symp.*, Memphis, TN, USA, Jul. 2014, pp. 259–260.

[26] Vaisala, "Sky condition algorithm for Vaisala ceilometer's," 2010. [Online]. Available: http://www.vaisala.com/Vaisala%20Documents/Brochures%20and%20Datasheets/Sky-Condition-CL31-Datasheet-B210507EN-B-LoRes.pdf

[27] Y. Liu and Y. Chen, "Precision of precipitable water vapour from radiosonde data for GPS solutions," *Geomatica*, vol. 54, no. 2, pp. 171–175, 2000.

[28] Y. Liu, "Remote sensing of atmospheric water vapor using GPS data in the Hong Kong region," Ph.D. dissertation, Dept. Land Surveying Geo-Informat., Hong Kong Polytechn. Univ., Kowloon, Hong Kong, 2000.

[29] T. V. Omotosho, J. S. Mandeep, and M. Abdullah, "Cloud-cover statistics and cloud attenuation at Ka- and V-bands for satellite systems design in tropical wet climate," *IEEE Antennas Wireless Propag. Lett.*, vol. 10, pp. 1194–1196, Oct. 2011.

[30] S. Dev, F. Savoy, Y. H. Lee, and S. Winkler, "WAHRSIS: A low-cost, high-resolution whole sky imager with near-infrared capabilities," *Proc. IS&T/SPIE Infrared Imaging Syst., Des., Anal., Model., Testing*, Baltimore, MD, USA, vol. 9071, May 2014, pp. 1–10.

[31] J. X. Yeo, Y. H. Lee, and J. T. Ong, "Site diversity gain at the equator: Radar-derived results and modeling in Singapore," *Int. J. Satell. Commun. Netw.*, vol. 33, no. 2, pp. 107–118, Mar. 2015.

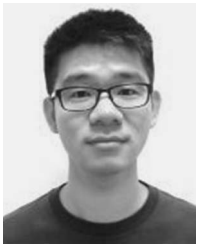

**Feng Yuan** (S'15) received the B.Eng. (Hons.) degree in electrical and electronics engineering from Nanyang Technological University, Singapore, in 2013, where he is currently working toward the Ph.D. degree with the School of Electrical and Electronic Engineering.

His current research interests include propagation, including the study of the effects of rain and cloud on the performance of satellite communication, and remote sensing of atmosphere.

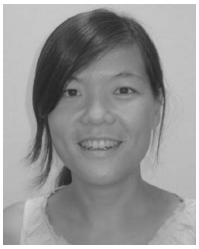

**Yee Hui Lee** (S'96–M'02–SM'11) received the B.Eng. (Hons.) and M.Eng. degrees from Nanyang Technological University, Singapore, in 1996 and 1998, respectively, and the Ph.D. degree from the University of York, York, U.K., in 2002.

She is currently an Associate Professor and an Assistant Chair (Student) with the School of Electrical and Electronic Engineering, Nanyang Technological University, where she has been a faculty member since 2002. Her research interests include channel characterization, rain propagation, antenna design, electromagnetic bandgap structures, and evolutionary techniques.

**Yu Song Meng** (S'09–M'11) received the B.Eng. (Hons.) and Ph.D. degrees in electrical and electronic engineering from Nanyang Technological University, Singapore, in 2005 and 2010, respectively.

From 2008 to 2009, he was a Research Engineer with the School of Electrical and Electronic Engineering, Nanyang Technological University. In 2009, he joined the Institute for Infocomm Research, Agency for Science, Technology and Research (A*STAR), Singapore, and later transferred to the National Metrology Centre, A*STAR, in 2011. From 2012 to 2014, he undertook a part-time secondment with Psiber Data Pte. Ltd., Singapore, where he was involved in the metrological development and assurance of a handheld cable analyzer, under a national Technology for Enterprise Capability Upgrading (T-Up) scheme of Singapore. He is currently a Scientist II with the National Metrology Centre, A*STAR. Concurrently, he is also a Technical Assessor with the Singapore Accreditation Council—Singapore Laboratory Accreditation Scheme in the field of radio frequency and microwave metrology. His current research interests include electromagnetic metrology, electromagnetic measurements and standards, and electromagnetic-wave propagations.

Dr. Meng is a member of the IEEE Microwave Theory and Techniques Society. He was a recipient of the national T-Up Excellence Award in 2015.

**Jin Teong Ong** received the B.Sc. (Eng.) degree from London University, London, U.K.; the M.Sc. degree from University College London, London; and the Ph.D. degree from Imperial College London, London.

From 1971 to 1984, he was with Cable & Wireless Worldwide PLC, Bracknell, U.K. He was an Associate Professor with the School of Electrical and Electronic Engineering, Nanyang Technological Institute (now Nanyang Technological University), Singapore, from 1984 to 2005 and an Adjunct Associate Professor from 2005 to 2008. From 1985 to 1991, he was the Head of the Division of Electronic Engineering. He is currently the Director of Research and Technology with C2N Pte. Ltd., Singapore, which is a company set up to provide consultancy services in wireless and broadcasting systems. His research and consultancy interests include antenna and propagation, particularly the system aspects of satellite, terrestrial, and free-space optical systems including the effects of rain and atmosphere; planning of broadcast services; intelligent transportation systems; EMC/I; and frequency spectrum management.

Dr. Ong is a member of the Institution of Engineering and Technology.